Natural recovery of infiltration capacity in simulated bank filtration of highly turbid waters

Gutiérrez, Juan Pablo; van Halem, Doris; Uijttewaal, Wim S.J.; del Risco, Efraín; Rietveld, Luuk C.

DOI
10.1016/j.watres.2018.10.009

Publication date
2018

Document Version
Final published version

Published in
Water Research

Citation (APA)
Gutiérrez, J. P., van Halem, D., Uijttewaal, W. S. J., del Risco, E., & Rietveld, L. C. (2018). Natural recovery of infiltration capacity in simulated bank filtration of highly turbid waters. *Water Research*, *147*, 299-310. https://doi.org/10.1016/j.watres.2018.10.009

Water Research 147 (2018) 299–310

Contents lists available at ScienceDirect

Water Research

journal homepage: www.elsevier.com/locate/watres

Natural recovery of infiltration capacity in simulated bank filtration of highly turbid waters

Juan Pablo Gutiérrez [a, b, *], Doris van Halem [a], Wim S.J. Uijttewaal [a], Efraín del Risco [c], Luuk C. Rietveld [a]

[a] Delft University of Technology, Faculty of Civil Engineering and Geosciences, Stevinweg 1, 2628CN, Delft, Netherlands
[b] Universidad del Valle, Cinara Institute, Faculty of Engineering, Calle 13 100-00, Cali, Colombia
[c] Universidad del Valle, Eidenar, Faculty of Engineering, Calle 13 100-00, Cali, Colombia

ARTICLE INFO

Article history:
Received 12 July 2018
Received in revised form
1 October 2018
Accepted 4 October 2018
Available online 8 October 2018

Keywords:
Infiltration recovery
Physical clogging
Riverbank filtration
Scouring
Self-cleansing
Turbidity

ABSTRACT

As a consequence of the suspended sediments in river water, cake formation on the streambed and clogging of the aquifer may occur, leading to a decline in the production yield of riverbank filtration systems, particularly in highly turbid river waters. However, naturally occurring flow forces may induce sufficient scouring of the streambed, thereby self-regulating the thickness of the formed cake layer. This study assessed the recovery of the infiltration capacity in a simulated physically clogged riverbank filtration system, due to self-cleansing processes. A straight tilting flume, provided with an infiltration column at the bottom, was used for emulating clogging, infiltration and self-cleansing. Based on the presented research it may be concluded that the infiltration of a mixture of different sediments, as found in natural water bodies, can already be recovered at low shear stresses. Clay and silt behaved very differently, due to the difference in cohesiveness. Clay was found to produce a persistent sticky cake layer, whereas silt penetrated deeper into the bed, both resulting in an absence of infiltration velocity recovery. A cake layer of fine sand sediments was easiest to remove, resulting in dune formation on the streambed. However, due to deep bed clogging by fine sand particles in a coarser streambed, the infiltration velocity did not fully recover. The interaction between mixed suspended sediments (5% clay, 80% silt, and 15% fine sand) resulted in uneven erosion patterns during scouring of the streambed and recovery of the infiltration velocity is low. Altogether it may be concluded that natural recovery of infiltration capacity during river bank filtration of highly turbid waters is expected to occur, as long as the river carries a mixture of suspended sediments and the sand of the streambed is not too coarse.

1. Introduction

Riverbank filtration (RBF) is a surface water treatment method for drinking water, using extraction wells located near the river in order to ensure direct aquifer recharge. As the surface water travels through the sediments, contaminants, such as pathogenic microorganisms, are removed (Schubert, 2003). RBF systems, like other filters, are, to some degree, vulnerable for clogging. Suspended particles in river water can affect the hydraulic conductivity of the bed and limit aquifer recharge (Caldwell, 2006). Streambed clogging may occur on the surface (external clogging) or within the porous media (internal clogging). Experience from the Netherlands has suggested that streambeds primarily consisting of gravels are at a far greater risk of clogging than those consisting primarily of finer grade materials (Stuyfzand et al., 2006). Also, the properties of the suspended particles in the river, such as particle size, affect the extent and clogging degree of the streambed and aquifer (Pavelic et al., 2011; Veličković, 2005).

External clogging corresponds to the cake build-up on the surface of the streambed due to the deposition of suspended solids, which reduces its permeability. Internal clogging, or deep bed clogging, occurs when the suspended particles enter the porous media and get stuck in the subsurface before abstraction (Du et al., 2014). Once a cake is built-up, penetration of particles into the porous media is prevented, and external – or cake clogging - rather than internal clogging will dominate (Fallah et al., 2012;

* Corresponding author. Delft University of Technology, Faculty of Civil Engineering and Geosciences, Stevinweg 1, 2628CN, Delft, Netherlands.
E-mail addresses: J.P.GutierrezMarin@tudelft.nl, juan.p.gutierrez@correounivalle.edu.co, juanpaguma@hotmail.com (J.P. Gutiérrez).

https://doi.org/10.1016/j.watres.2018.10.009
0043-1354/

Sacramento et al., 2015). Cake and deep bed clogging may also happen simultaneously (mixed clogging), caused by the movement of particles within the porous media and the accumulation of sediments in the upper layer (Du et al., 2014). With this mixed clogging, the hydraulic conductivity of the soil decreases over time, but it decreases much faster in the top layer (Du et al., 2014). Cake clogging may be reversible, but this is typically not the case for deep bed clogging (Pholkern et al., 2015; Seiler and Gat, 2007).

Physical, mechanical, chemical and biological clogging are the main obstruction mechanisms occurring in the streambed. The physical clogging occurs when inorganic and organic suspended solids in the river (e.g., clay, silt particles, algae cells, microorganisms, flocs) become trapped in the streambed pore channels as water flows from the river and through the aquifer (Bouwer, 2002; Caldwell, 2006; Hubbs, 2006a; Pavelic et al., 2011; Schubert, 2002). Particle size distribution and suspended solids concentration in the river water are considered the main factors affecting the physical clogging process (Blaschke et al., 2003; Bouwer, 2002; Pavelic et al., 2011; Platzer and Mauch, 1997). Mechanical clogging refers to air entrainment during recharge from vadose zone to the phreatic aquifer or gas binding from microbiological activities (e.g., methane) (Martin, 2013). Chemical clogging is the loss of hydraulic conductivity of the streambed due to the precipitation of initially soluble water constituents, due to changes in redox potential and pH values caused for example by mixing with native groundwater (e.g., carbonate precipitates, iron hydroxides) (Bouwer, 2002; Caldwell, 2006). The accumulation of precipitates in pores might lead to chemical clogging in the aquifer and nearby the abstraction well (Schubert, 2002). Biological clogging is caused by the accumulation of bacterial cells in the streambed (Baveye et al., 1998; Bouwer, 2002; Engesgaard et al., 2006). The growth of these bacterial cells is dependent on physical-chemical factors associated with both soil and water (Pavelic et al., 2011).

Naturally occurring flow forces may induce sufficient scouring of the streambed, thereby self-regulating the thickness of the formed cake layer and restoring its hydraulic conductivity. Vertical sedimentation forces induce the deposition of particles on the streambed. Horizontal forces onset the resuspension of the deposited particles. The extent of scouring is determined by the magnitude of the shear stress and the properties of the streambed and cake layer, deposited onto the streambed. Scouring or self-cleansing capacity of RBF systems is commonly assessed in terms of streambed particle size (considering critical shear stress) and the shear stress exerted by the river flow. Reported shear stress values typical for river streambeds range between 1 and 100 N/m^2, considering a value of 20 N/m^2 as reasonable (Hubbs, 2006b). However, van Rijn et al. (2007) reported shear stress values for individual sediments ranging from 0.08 to 0.4 N/m^2. The shear stress for the mobilization in porous media of colloidal particles, such as clay, have been reported to range from 0.1 to 1 N/m^2 (Manga et al., 2012; Mays, 2013). Thus, the incipient motion of sediments depends on critical shear stress, which is a function of streambed-armor layer characteristics. For particles finer than 62 μm, the critical shear stress increases as particle size decreases due to the cohesive effects (van Rijn et al., 2007).

Erosion and deposition exhibit dissimilar behavior for cohesive and non-cohesive sediments (Winterwerp and van Kesteren, 2004). Cake layers composed from the deposition of cohesive materials, carried by the rivers, will increase the resistance to erosive processes, meaning higher shear stresses to move the sediments deposited on the streambed. In addition, cohesive sediments have a different shear stress for deposition than for erosion (Krishnappan, 2007). The cake layer may affect the surface water/groundwater interaction and therefore may influence the abstraction capacity yield by altering the permeability of the streambed (Packman and MacKay, 2003). The mechanisms affecting the infiltration velocity based on the movement and settlement of particles on streambeds and the streambed–aquifer clogging are represented in Fig. 1.

The streambed infiltration velocity (q) thus depends on the characteristics of the streambed sediments and the suspended sediments being transported by the river, and it is expected to vary according to the characteristics of the flow (i.e., streambed velocity and flow velocity profile across the river), leading to the deposition and resuspension of particles. The minimum shear stress, τ_c, is defined by the gravitational and cohesive forces that resist particle motion in ideal conditions. When the friction velocity on the sediment bed is greater than the threshold velocity, sediment particles on the bed will become mobilized. The variables that influence the infiltration velocity in the porous media considering the clogging and self-cleansing processes are (e.g., Cunningham et al., 1987; Wang, 1999; Winterwerp and van Kesteren, 2004; Huang et al., 2006; Pugh, 2008; Al-Madhhachi et al., 2013; Zheng et al., 2014): initial infiltration velocity (q_o), density of the fluid (ρ_w) and suspended particles (ρ_s), dynamic viscosity of the water (μ), suspended particle diameter (d_s), d_{50} particle size of the streambed media, surface water depth, bed slope, flow velocity (u), suspended particle concentration ($\varnothing_{sed}$), porosity of streambed, and particle attachment and detachment coefficients.

The main purpose of this study is to evaluate the effect of the concentration of suspended solids and different compositions of the suspension on physical clogging and recovery of the infiltration capacity by subsequent self-cleansing for highly turbid waters. To the authors' knowledge, this has not yet been studied previously. To achieve this, physical modeling with an experimental RBF set-up was conducted in order to assess the effect of flow velocity, particle size of the streambed media, suspended particle diameter, and suspended particle concentration on the infiltration velocity during clogging and self-cleansing. Special attention was paid in this study to differentiate between cake and deep bed clogging.

2. Materials and methods

2.1. Experimental setup

A straight tilting flume with two channels (duplicate) was used for simulation of the river flow (Fig. 2). Infiltration columns placed at the bottom were used to determine the effect of variable shear stress conditions on self-cleansing and infiltration. The channels had dimensions of 500 cm length by 19 cm width and were constructed of smoothed wood. The lateral walls were made of wood and Plexiglas. The infiltration columns were made of transparent Plexiglas (50 cm long and 10.8 cm ID). The columns were equipped with four piezometers for the monitoring of head loss over the height of the porous media and four sampling ports (placed 10 cm from each other). The bottom of the channels was roughened by gluing 0.2–0.8 mm sand onto them, leaving the sides smooth. Flow characteristics were measured with an electromagnetic flowmeter (EM). Turbidity was measured at the different ports of the columns using a turbidity meter (HACH 2100P). The infiltration velocity ($q = Q/A$, where $Q = V/t$ and A is the area of column perpendicular to the water flow) and pressures were monitored for the duration of the experiments to assess porous media clogging and infiltration recovery. The experiments were conducted at room temperature (about 20 °C).

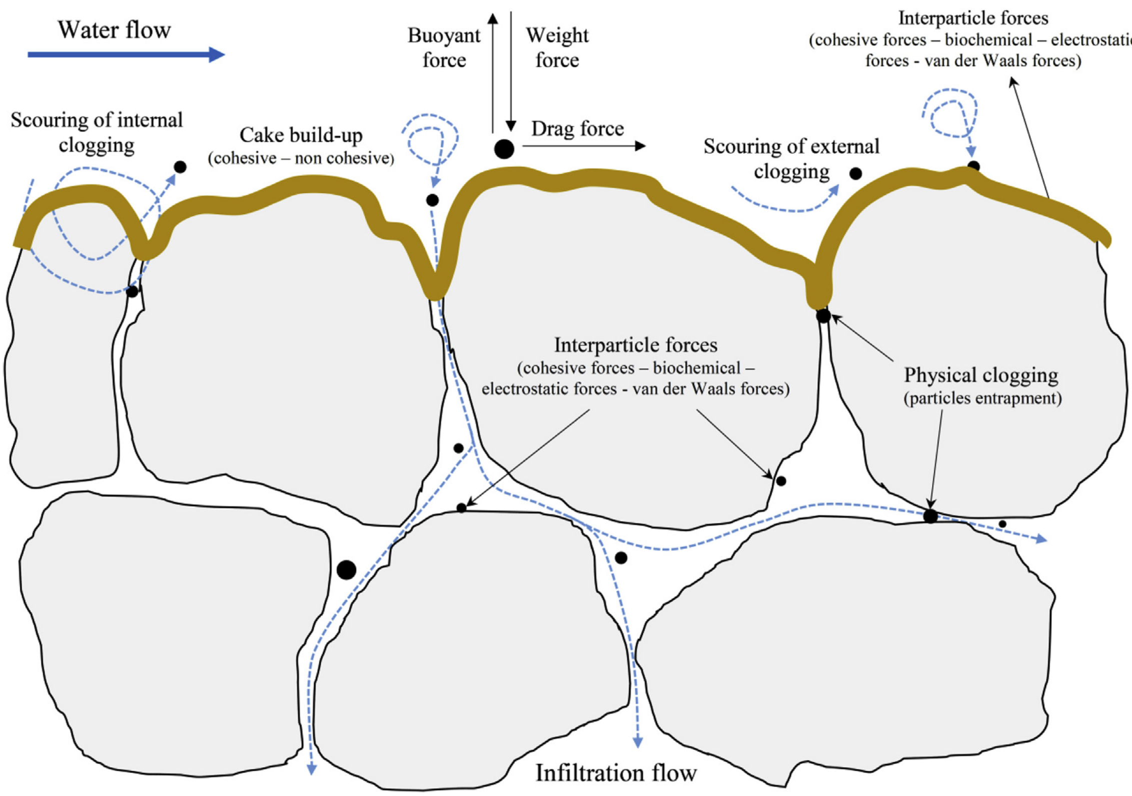

Fig. 1. Mechanisms influencing infiltration velocity related to streambed clogging and self-cleansing processes.

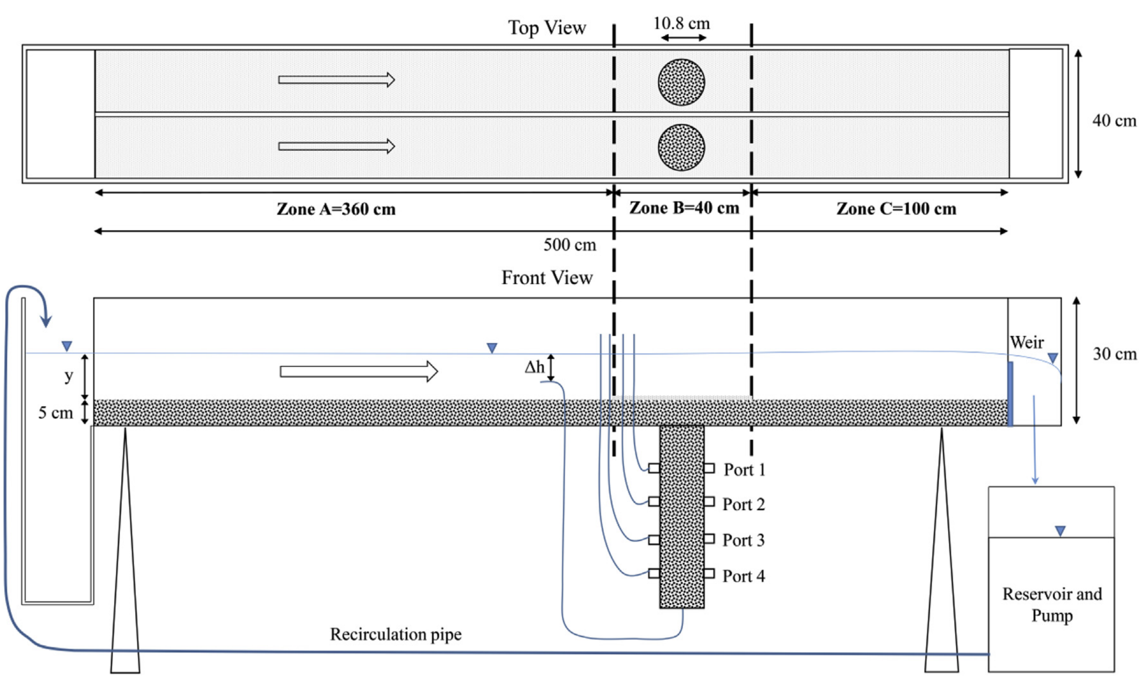

Fig. 2. Scheme of the experimental setup.

2.2. Sediments

2.2.1. Suspended sediments

The suspended sediments were selected based on characteristics of the natural sediments identified in a highly turbid river (Cauca River in Cali, Colombia) (Gutiérrez et al., 2016), where particle size distribution and specific surface was determined by wet laser diffraction instrument (Model Hydro, 2000SM, Malvern). Sediment properties for dry and rainy conditions are summarized in Table 1.

Table 1
Properties of natural suspended sediments, Cauca River in Cali, Colombia (Gutiérrez et al., 2016).

	Dry conditions (*n=18*)						Rainy conditions (*n=8*)					
	d_{s_10} (μm)	d_{s_50} (μm)	d_{s_90} (μm)	Clay (%)	SOM (g/kg)	PI (%)	d_{s_10} (μm)	d_{s_50} (μm)	d_{s_90} (μm)	Clay (%)	SOM (g/kg)	PI (%)
Mean	7.2	25.6	125.7	0.57	0.38	15.5	5.3	23.0	85.3	4.24	0.62	26.0
Min	4.8	17.9	64.1	0.23	–	–	3.8	17.2	74.7	2.88	–	–
Max	10.3	36.2	264.1	1.67	–	–	6.9	26.8	91.8	6.20	–	–
SD	1.3	4.7	55.8	0.38	–	–	1.0	3.5	5.9	1.19	–	–

SOM: soil organic matter PI: plasticity index.

Considering the characteristics described in Table 1, the whole sample of sediments collected in the Cauca River may be regarded as inorganic - non-cohesive. Therefore, inorganic fine sediments were used to simulate the natural suspended sediments in the Cauca River: IMERYS Polwhite E clay (0.5–10 μm, $d_{s\_50} = 3.5$ μm), M300 silt from Sibelco (3–40 μm, $d_{s\_50} = 17$ μm), and S90 fine sand from Sibelco (63–180 μm, $d_{s\_50} = 150$ μm). The IMERYS Polwhite E corresponds to the clay + very fine silt subclass as classified by the American Geophysical Union.

2.2.2. Streambed material

Three streambed/aquifer configurations were used: (1) streambed and columns from coarse sand from Sibelco (1.0–1.6 mm, $d_{50} = 1.36$ mm); (2) streambed from medium sand from Sibelco (0.2–0.8 mm, $d_{50} = 0.61$ mm) and columns from coarse sand (1.0–1.6 mm, $d_{50} = 1.36$ mm); and (3) streambed and columns from medium sand (0.2–0.8 mm, $d_{50} = 0.61$ mm). The grain sizes were selected in order to emulate an alluvial formation based on the characteristics found in the Cauca River section next to the main water treatment plant of the city of Cali, Colombia (CVC and Universidad del Valle, 2004a).

2.3. Experimental procedure

The experiments consisted of two subsequent phases: (1) clogging of Zone B (see Figs. 2 and 3), followed by (2) scouring conditions flowing from Zone A to Zone C. The clogging experiments of the streambed in Zone B were conducted for two sediment concentrations (1 g/L and 6 g/L), an initial infiltration velocity of 6 m/d, and two streambed media ($d_{50} = 0.61$ mm and $d_{50} = 1.36$ mm). After packing the columns, the soil was saturated from the bottom up with tap water, which was pumped at a 2 mL/min constant flow with a peristaltic pump (Watson-Marlow Sci-Q 205S/CA). The bottom of the column was connected to a saturated tube discharging to the atmosphere at an elevation above the top of the streambed but below of the water level in the channel (Figs. 2 and 3).

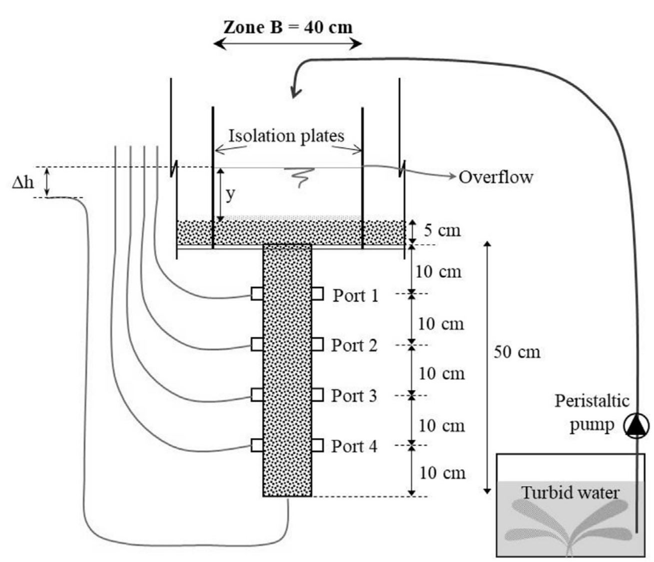

Fig. 3. Scheme of set up for clogging experiments.

The scouring experiments were carried out with tap water at different shear stresses. Physicochemical characteristics of the tap water used during the experiments from seven water samples were: pH = 7.9–8.0, ionic strength = 0.00724 ± 0.00038 mol/L and sodium adsorption ratio (SAR) = 1.216 ± 0.041. The data of the samples was provided by the water company of Delft, the Netherlands (Evides Waterbedrif). The pH of tap water used is similar to the pH found in the Cauca River (6.5–7.5) (CVC and Universidad del Valle, 2004b).

As mentioned before, IMERYS Polwhite E (kaolinite) was used for representing the clay fraction of the suspended sediments. For kaolinite, at similar pH and SAR conditions as the used tap water, critical coagulation concentrations of about 0.5–0.7 $mmol_c$/L have been reported (Goldberg et al., 1991).

2.3.1. Streambed critical shear stress

The shear stress is the force of moving water against the streambed of the channel ($\tau = \rho_w ghS$, where g is the gravitational force, h is the water depth in the channel and S is the water surface slope). The shear stress for incipient motion of the streambed material was determined by placing 5-cm height of the streambed material (Fig. 2) onto the flume bottom and then moving water at different bed slopes and flows (different shear stresses) until bed movement occurred. The shear stress in the flume that resulted in bed movement was established as the critical shear stress (τ_c) for the clean streambed. A 14-cm constant water level (h) during the experiments was maintained by using an adjustable weir at the downstream end of the flume and by modifying the water discharge and the flume slope.

2.3.2. Clogging experiments

Turbid influent water (Fig. 3) was pumped into the flume from a reservoir. Zone B was isolated from the rest of the flume by wooden plates in order to clog solely this region and the infiltration column. During the clogging experiments, the turbid solution in the reservoir was thoroughly mixed during the whole experiment. Additionally, the entering turbid solution in Zone B was continuously mixed by using a four-bladed propeller stirrer placed at the upper zone of the water level at a velocity fast enough to achieve a uniform particle distribution and slow enough to allow the deposition of particles and avoid the disturbance of the bed. The water level in Zone B was controlled by using a laser sensor (optoNCDT 1302).

Synthetic turbid solutions were infiltrated into the columns (1 g/L and 6 g/L). An initial filtration velocity 6 m/d was used, based on values reported in the literature for RBF systems (Dawe, 2006; Hubbs, 2006a). The initial filtration velocity was achieved by maintaining a constant head (Δh) between the water level in the flume and the outlet level in the columns (Fig. 3). In addition to the different tested concentrations, four different suspended particle sizes were used to prepare the turbid solutions: (1) clay 0.5–10 μm, $d_{s\_50} = 3.5$ μm; (2) silt 3–40 μm, $d_{s\_50} = 17$ μm; (3) fine sand 63–180 μm, $d_{s\_50} = 150$ μm; and (4) mixed clay, silt and fine sand 0.5–180 μm. The mixed material was comprised of 5% clay, 80% silt and 15% fine sand, in agreement with the composition of the sediments in the Cauca River (Gutiérrez et al., 2016).

The experiments ran for periods between 24 and 168 h, depending on the sediment concentration. The pressure was continuously monitored through the piezometers during the experiments. Water samples (15 mL) were extracted from each sampler port by using a multichannel peristaltic pump (Watson-Marlow Sci-Q 205S/CA) at a slow flow rate (1 mL/min) per channel in order to avoid disturbances of the porous media and deposited sediments. Turbidity values were determined through a portable turbidimeter (2100Q from HACH). Tap water was used to prepare the turbid solutions that were continuously stirred in order to ensure their homogeneity. The height of the cake layer was continuously measured by using a metric ruler, taped to the transparent Plexiglas wall (Zone B).

2.3.3. Infiltration and self-cleansing experiments

Movable bed conditions were used in Zones A, B, and C of the flume (Fig. 2). Zone A had a 360-cm length, designed to achieve a fully-developed fluid flow. Zone B had a 40-cm length, including the 10.8-cm diameter of the column. Zone C had a 100-cm length, designed to observe the deposition and resuspension of sediments. Zones A, B, and C were covered with 5-cm of the streambed material.

Self-cleansing was assessed based on the threshold Shields parameter, θ_c, which is a non-dimensional number indicating the initiation of sediment transport in channels. The θ_c was calculated from the experimentally determined critical shear stress, τ_c, found in equation (1), and verified from the theoretical equation (2) by Soulsby and Whitehouse (1997),

$$\theta_c = \frac{\tau_c}{g(\rho_s - \rho_w)d_{50}} \tag{1}$$

$$\theta_c = \frac{0.3}{1 + 1.2D_*} + 0.055[1 - \exp(-0.02D_*)] \tag{2}$$

Where the dimensionless grain size, D_*, is defined as

$$D_* = \left[\frac{g((\rho_s/\rho_w) - 1)}{(\rho_w/\mu)^2}\right]^{1/3} d_{50} \tag{3}$$

Three Shields parameters (θ) were evaluated (approximately $0.5\theta_c$, θ_c, $2\theta_c$ depending on the bed particle size) during the self-cleansing experiments. The assessed θ values were selected based on both the experimentally determined τ_c and the calculated threshold Shields parameter for each streambed. Both, the experimentally determined (applying eq. (1)) and theoretically calculated (applying eq. (2)) τ_c gave values of 0.72 and 0.66 N^2/m for $d_{50} = 1.36$ mm and $d_{50} = 0.61$ mm, respectively. Julien (1998) reported values between 0.47 and 1.3 N/m^2 and 0.27–0.47 N/m^2 for very coarse sand (1–2 mm) and coarse sand (0.5–1 mm), respectively. In order to make the experiments comparable, three shear velocities ($u_* = \sqrt{\tau/\rho_w}$) were assessed (0.017 m/s, 0.029 m/s and 0.041 m/s), corresponding to flow velocities in the channels ($u = Q/A$, where Q is the volumetric flow in the channel and A is the transversal area to the water flow) of 0.318 m/s, 0.327 m/s and 0.342 m/s, respectively, for both streambeds considering critical Shields parameters ($\theta_c = 0.034$ and 0.031 for $d_{50} = 1.36$ mm and $d_{50} = 0.61$ mm, respectively). Julien (1998) reported values from 0.029 to 0.039 and 0.029 and 0.033 for very coarse sand (1–2 mm) and coarse sand (0.5–1 mm), respectively. Each streambed velocity was applied during approximately 3 h, in order to avoid the interference from ripples and dunes formations in Zone B. Specific discharges and water pressures were monitored in the infiltration columns as indicators of clogging.

3. Results

3.1. Cake and deep bed clogging

3.1.1. Cake layer formation

Fig. 4a presents the variations in the cake layer formation rate (mm cake height per suspended sediment load, mg ($Q\varnothing_{sed}t$, where t is time)) for different suspended sediment sizes, d_s, and under two different suspended sediment concentrations, $\varnothing_{sed}$.

From Fig. 4a it can be observed that the fastest cake formation occurred when passing clay through the porous media. In addition, for all the suspended sediments, except for clay, a higher cake layer formation rate occurred at the lower sediment concentration. The cake layer formation rate is given as mm/mg sediment load, and therefore not related to time, which means that, although at higher sediment concentration the cake layer formation is faster the relative, contribution of passing suspended sediments to cake layer

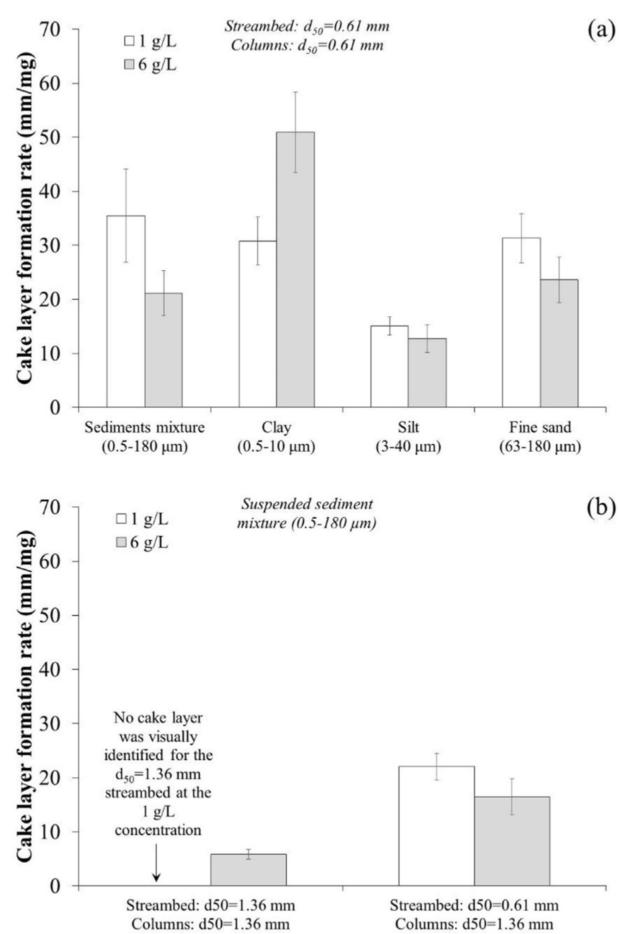

Fig. 4. Cake layer formation rate as a function of (a) suspended sediment size and (b) streambed particle size; both for 1 and 6 g/L suspended sediment concentration. The top line represents the arithmetic mean. The whiskers extend to the standard error.

formation is smaller, except for clay.

The cake layer formation rate as a function of the streambed particle size is presented in Fig. 4b. A higher cake formation rate for the same streambed-column configuration (streambed: $d_{50} = 0.61$ mm, columns: $d_{50} = 0.61$ mm) than for the different streambed-column configuration (streambed: $d_{50} = 0.61$ mm, columns: $d_{50} = 1.36$ mm) was observed. For the large streambed particle size ($d_{50} = 1.36$ mm), no cake layer was formed for the low sediment concentration of 1 g/L. For the fine streambed particle size ($d_{50} = 0.61$ mm), a higher cake layer formation velocity occurred at the low sediment concentration.

3.1.2. Deep bed clogging

Turbidity measurements were done over the column height as indicator for assessing deep bed clogging. The values shown in Fig. 5 correspond to the average of samples withdrawn each 3–4 h during the run of each experiment. The water containing clay particles (0.5–10 µm) presented the lowest turbidity measurements over the column heights for both sediment concentrations. For the silt-size particles (3–40 µm) at the higher sediment concentration (6 g/L), the turbidity increased as the travel distance increased. The turbidity for both sediment concentrations and both streambed particle sizes over the column height is illustrated in Fig. 5. For the larger streambed particle size ($d_{50} = 1.36$ mm) the turbidity was stable over the height of the column with an average of 6.3 NTU and 31.9 NTU for 1 and 6 g/L, respectively. For both sediment concentrations higher turbidity values were observed in the top 35 cm of the column with the smaller streambed particle size ($d_{50} = 0.61$ mm) than with the larger streambed particle size ($d_{50} = 1.36$ mm).

In Fig. 6 the permeability, k, changes per each segment of the columns are shown as relative permeabilities (k between ports divided by the clean-bed permeability, k_o) as a function of the injected sediment load. As observed in Fig. 6, the higher permeability reduction occurred in the first 15 cm (top layer) for all the suspended sediment sizes tested, which is linked to cake clogging. This happened faster at the lower suspended sediments concentration. Deep bed clogging, represented by the permeability reduction in the lower segments, was evidenced for all sediment sizes, being higher as the particle size decreased (clay > silt > fine sand). For fine sand, the top layer was not clogged, nor deep bed clogging was observed at the higher suspended sediment concentration (Fig. 6c). The mixture of suspended sediments presented the highest and fastest cake clogging occurrence, and the lowest deep bed clogging (except for fine sand).

3.2. Infiltration velocity during clogging

Fig. 7 presents the variations in the infiltration velocity for different turbid solutions in relation to the infiltrated sediment mass ($(q - q_o)/Q\varnothing_{sed}t$) (in m/d/mg). This infiltration velocity decline was higher for a sediment concentration of 1 g/L, compared to 6 g/L, apart for clay. This is in-line with the faster development of cake layer at 1 g/L (velocity expressed per sediment load). It must be taken into account that the analysis was realized using suspended sediment load instead of time to make them comparable. For fine sand, no reduction of the infiltration velocity occurred at 6 g/L, whilst a slight reduction was observed for 1 g/L.

In Fig. 7b, the changes in infiltration velocities are compared for two streambed particle sizes ($d_{50} = 1.36$ mm and $d_{50} = 0.61$ mm), where the column particle size was the same for both ($d_{50} = 1.36$ mm). The mixture of suspended sediments was used for this experiment. Higher infiltration velocity decline per weight of sediment load was observed at the lower sediment concentration. When comparing the infiltration velocity decline for mixed sediments in the same particle sizes for both column and streambed

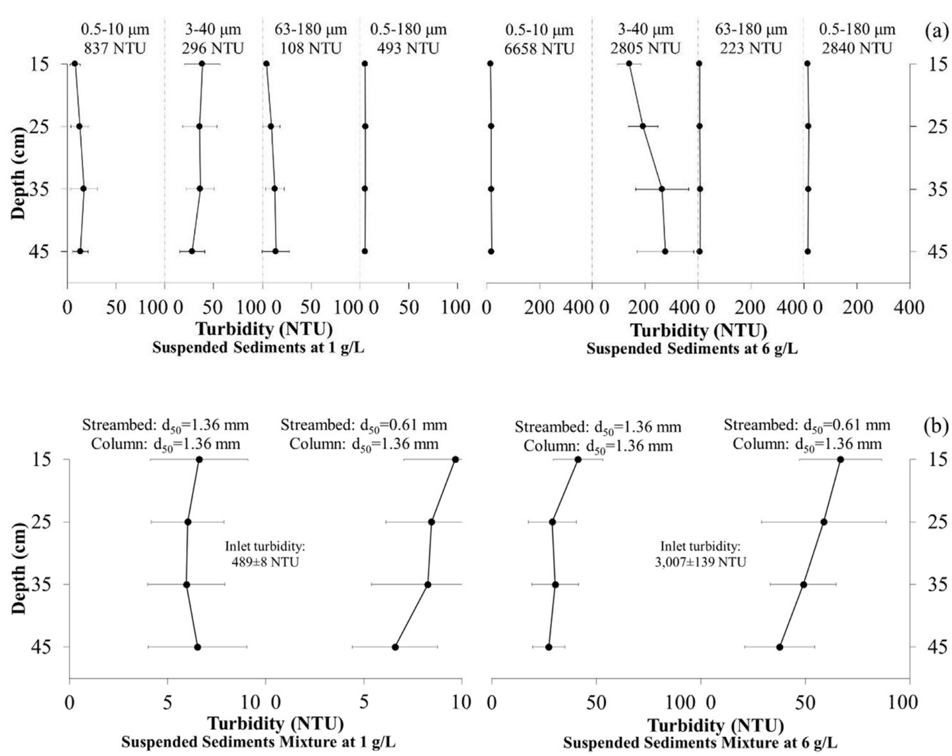

Fig. 5. Turbidity at different column heights as a function of (a) suspended sediment size and (b) streambed size. The point represents the arithmetic mean of the samples. The whiskers extend to the standard deviation.

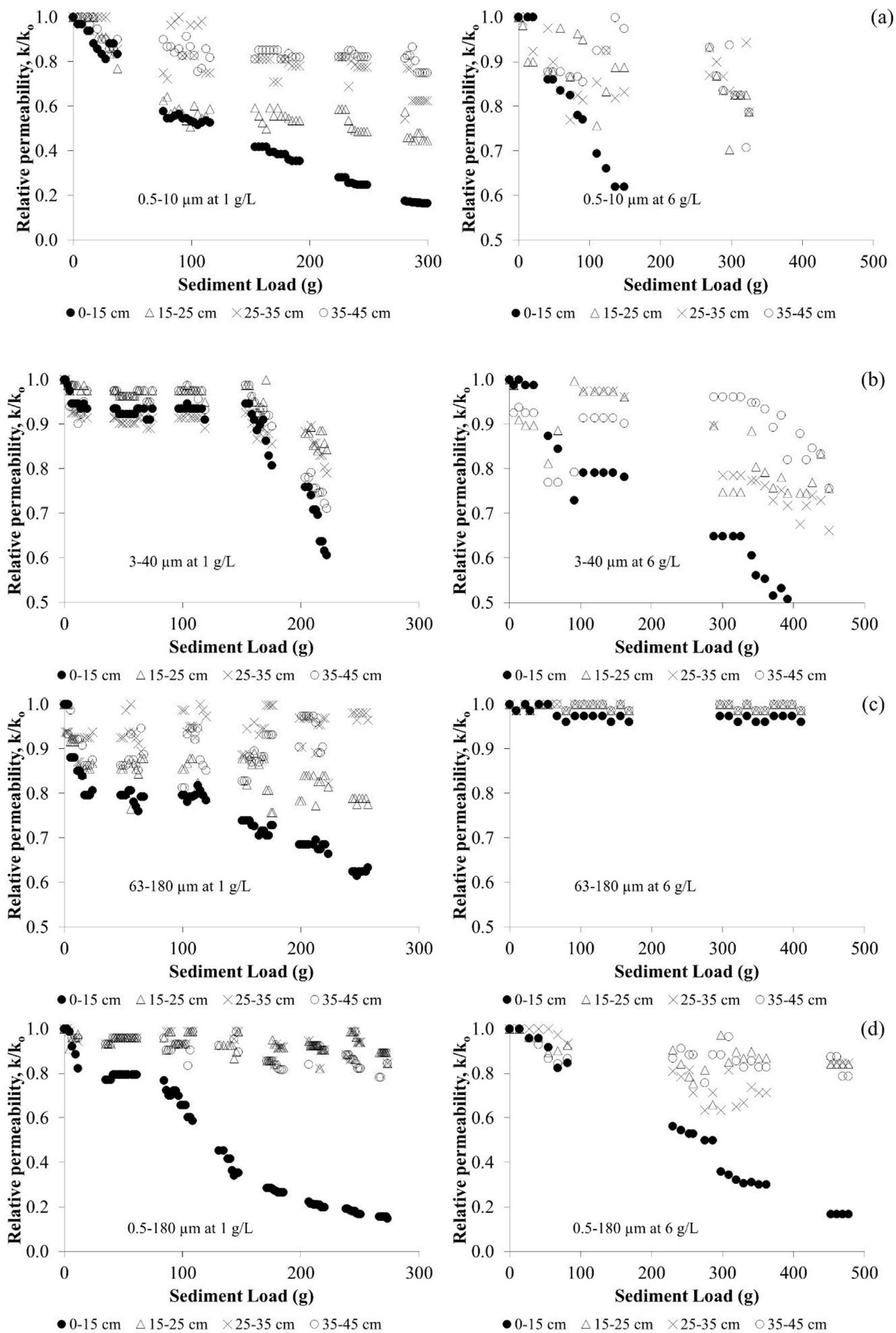

Fig. 6. Relative permeability as a function of sediment load into (a) clay, (b) silt, (c) fine sand and (d) mixed sediments for different sediment loads of 1 g/L (left) and 6 g/L (right). Note the different relative permeability ranges featured on each axis.

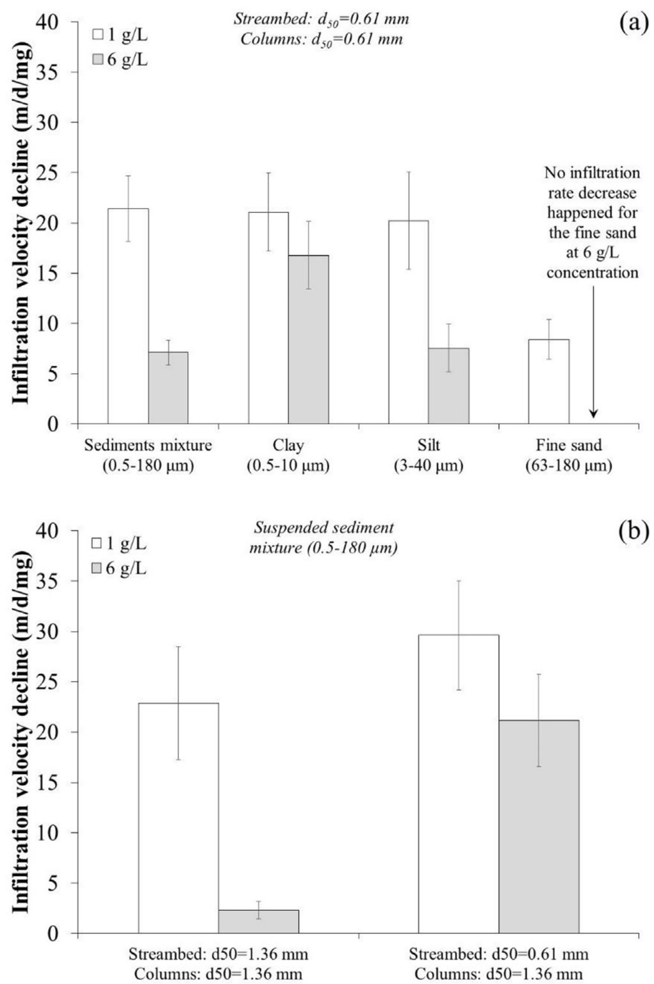

Fig. 7. Infiltration velocity decline as a function of (a) suspended sediment size and (b) streambed particle size. The top line represents the arithmetic mean. The whiskers extend to the standard error.

($d_{50} = 0.61$ mm) versus different particle sizes (streambed $d_{50} = 0.61$ mm; columns $d_{50} = 1.36$ mm), a much larger infiltration velocity decline was obtained for the different particle sizes.

3.3. Cake layer scouring

The removal of the cake layer by scouring forces was registered during the assessment of three Shields parameters (θ): $0.5\theta_c$, θ_c, and $2\theta_c$, compared to no flow with $\tau_c = 0$ and subsequently $\theta = 0$. The shear velocities were of 0.017, 0.029 and 0.041 m/s, respectively. The tests were conducted for the medium sand streambed ($d_{50} = 0.61$ mm). Fig. 8 illustrates the cake layer removal as a function of streambed velocities for the cake layers composed of different suspended sediments. For the experiments conducted with clay particles (0.5–10 μm), a relatively high removal (32–46%) of the cake layer was observed at $\theta = 0.5\theta_c$. However, little additional cake layer was being removed at $\theta = 1$ and no extra removal was observed at $\theta = 2\theta_c$. At the higher sediment concentration, a much thicker cake layer was formed, which also resulted in a thicker remaining clay layer after scouring (8 mm). Compared to clay, the cake layer made of silt (3–40 μm) was consistently harder to remove, though at each increased shear stress a fraction of the layer was removed. Most silt particles from the removed cake layer were re-suspended in the water, but it was also observed that silt

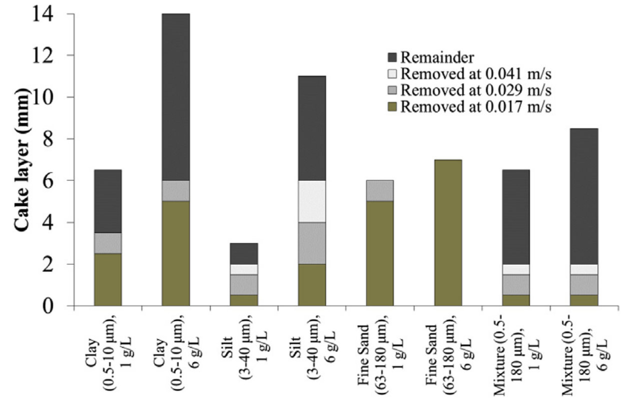

Fig. 8. Cake layer scouring for different suspended sediment sizes.

particles were partly re-settled in the subsequent Zone C (Fig. 2). The re-settlement suggests a potential clogging effect downstream the evaluated zone. At the same time, the newly-cleaned streambed may become clogged with material scoured upstream. For the fine sand cake layer (63–180 μm), most of the deposited sediments were easily removed at the lower streambed velocity as observed in Fig. 8. Although, the fine sand sediments were moved from their initial position, the formation of ripples and dunes were observed in Zone C. As a consequence, scouring of the original streambed was also onset ($d_{50} = 0.61$ mm). The cake layer formed by the mixture of sediments presented the highest resistance to erosion of all the suspended sediments assessed, with only 23–31% of the cake layer being removed.

3.4. Infiltration velocity after scouring

Fig. 9 compares the recovery of the infiltration velocity during the self-cleansing experiments. Relative infiltration velocities as a function of the initial infiltration velocity (q/q_0), i.e., at clean bed conditions, are shown. The results for $\theta_c = 0$ correspond to the infiltration velocity of the clogged streambed, before starting the self-cleansing experiments. In none of the experiments, independent of suspended sediment type or concentration, the infiltration velocity recovered to its initial capacity regardless of the bed shear stress applied.

Although the remainder of the cake layer after bed scouring was the thickest for the mixed suspended sediments (Fig. 8), comparable to the clay layer, the flow velocity recovery was the highest (84–96%) for the mixed suspended sediments at both concentrations compared to the uniform suspended sediment sizes (Fig. 9a). During the clogging experiments with the mixed suspended sediments, cake layer cracks were observed. For the lower suspended sediments concentration, the recovery was higher even if the infiltration velocity reduction during the clogging experiment was high (Fig. 7). Though the cake layer of the largest uniform suspended sediment sizes (fine sand, 63–180 μm) was completely removed for both concentrations, no recovery of the infiltration velocity was obtained. As observed in Fig. 9b, no differences in the infiltration recovery existed between both streambed sizes at the lower concentration. On the other hand, a higher infiltration capacity occurred for the smaller streambed size ($d_{50} = 0.61$ mm) at the higher suspended sediment concentration, which may be explained by movement of the original streambed as cracking of the cake layer was observed.

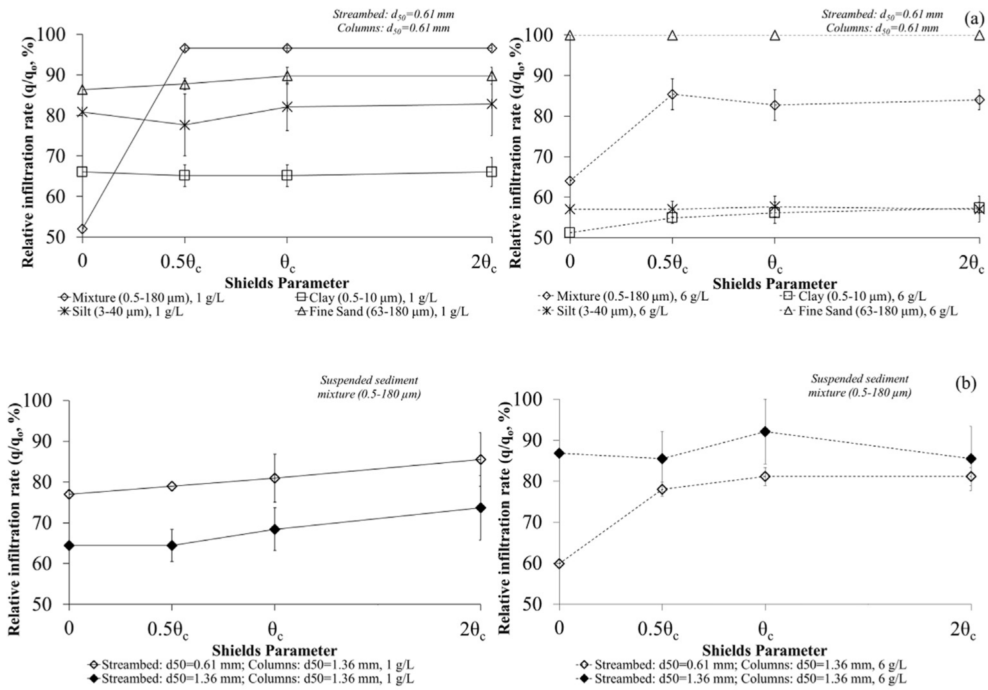

Fig. 9. Infiltration velocity recovery as a function of Shields parameter at different clogging conditions: (a) after clogging at 1 g/L and (b) after clogging at 6 g/L. The point represents the arithmetic mean of the samples. The whiskers extend to the standard deviation.

4. Discussion

4.1. Cake clogging or deep bed clogging

When comparing the different types of suspended sediments, deep bed clogging was observed most predominantly for the experiments with silt. The low cake formation velocity and the high infiltration velocity decline for silt particles at the higher suspended sediments concentration is linked to the non-cohesive nature of the silt (Winterwerp and van Kesteren, 2004), where, the weakness of physicochemical processes limits the attachment of silt particles to each other and onto the sand particles. Therefore, the entrapped particles can be easily remobilized by the water flow reaching lower layers, leading to deep bed clogging. The clay particles were found to be mostly retained in the cake layer, which may then be explained by the cohesiveness of clay particles (Krishnappan, 2007). The cohesive nature of clay leads to particles aggregation of clay sediments (floc formation), particularly at high concentrations (Klassen et al., 2013). Therefore, although both turbidity values tested during this research were high (1 g/L and 6 g/L), the findings show that the 1 g/L suspended solids led to higher cake layer formation velocities for non-cohesive particles, while 6 g/L suspended solids concentration was favorable for higher cake layer formation velocities in cohesive particles, having the opposite effect on the formation of deep bed clogging.

The suspended sediments mixture pinpoints the effect of the interparticle forces acting among the sediments (e.g., van der Waals) and the interaction between them and the bed particles, leading to larger particles with the ability to be retained on the top layer (cake filtration) due to the clay content. Also, the interaction amongst different suspended particles onsets new clogging mechanisms, e.g.: (1) entrapment and sedimentation of fine sand sediments in small voids, (2) entrapment of silt particles in existing voids and new voids because of the trapped fine sand, and (3) straining, hydrodynamic bridging and interparticle forces of clay and the retained suspended sediments (Veličković, 2005). When reviewing the cake layer and deep bed turbidity measurements (Figs. 4 and 5), the fine sand behaved very similar to the mixed sediments. Nevertheless, the low infiltration velocity reduction for the fine sand experiments reveals that although the cake layer may have had the same thickness, it was more permeable than is the case for mixed sediments.

Different clogging mechanisms influence the infiltration capacity reduction in relation to the streambed size. The smaller voids due to the smaller bed particle size are likely to retain more suspended sediment particles by entrapment (Winterwerp and van Kesteren, 2004). In this case mixed bed clogging occurs, where cake clogging plays the most important role in the precluding of the water passage through the media as reported for slow sand filtration (Grace et al., 2016). On the other hand, deep bed clogging is the dominant mechanism for the large streambed size. The larger voids have a larger storage capacity for particles, and then enhance the mobility of particles into the media before clogging (Veličković, 2005), favoring deep bed clogging occurrence. This behavior has been widely reported for rapid sand filtration, where suspended and colloidal particles are depth filtered (Ripperger et al., 2012). The presence of larger voids can enhance the mobility of fine particles because of the higher flow velocities leading to higher hydrodynamic forces and to the weaker interparticle bonding forces (Jacobsen et al., 1997; Reddi et al., 2000). The weak support exerted by the filling material of the columns, which, being larger than the particles of the streambed, was not able to retain the particles previously entrapped, and due to the changes in flow velocities between the transition from $d_{50} = 0.61$ mm (streambed) to $d_{50} = 1.36$ mm (column) contributed to sudden releases of particles.

4.2. Self-cleansing of cake layer

As stated by various researchers, bed scouring depends on streambed particle size (Caldwell, 2006; Stuyfzand et al., 2006). The

Table 2
Overview of cake layer removal and infiltration velocity recovery per sediment type.

Sediment type	Sediment concentration (g/L)	Cake layer removal (mm)	Average infiltration velocity recovery 0.5-2θ_c (m/d)			Average infiltration velocity recovery 0.5-2θ_c (q/q_o, %)
			q_o	q after clogging	q after scouring	
Clay	1	6.5	8.8	5.82	5.82	66.1
	6	14	6.45	3.30	3.69	57.3
Silt	1	3	6.09	4.92	5.03	82.6
	6	11	6.13	3.50	3.50	57.0
Fine sand	1	7	5.78	4.99	5.185	89.7
	6	6.5	5.86	5.86	5.86	100.0
Mixture	1	6.5	5.74	2.99	5.54	96.5
	6	8.5	5.90	3.78	4.95	84.0

suspended particle type has demonstrated to be the most important variable governing the self-cleansing of the streambed for an uncovered, clean streambed (e.g., absence of plants, biofilm). The initial high removal velocity found with the cake layer made of clay may be referred as entrainment and/or floc erosion. The absence of additional removal may be related to the interaction strength between the sandy bed and the mud (clay) layer due to the cohesive and adhesive characteristics of the clay, leading to a much higher erosion threshold (Jacobs et al., 2011). However, it must be noted that a recirculating flume was used during the experiments. Thus, the resuspended clay conveyed to a turbidity current, which could have affected the cake layer erodibility by the so-called hindered erosion (Winterwerp and van Kesteren, 2004). The much thicker cake layer formation obtained at the higher suspended sediments concentration highly impacted the initial scouring of the clay cake. This is related to the lower cake layer compression on the top layer and therefore a weaker strength to erosion (Mahdi and Holdich, 2013; Mays and Hunt, 2005). The non-cohesive nature of silt leads to a weak interaction between the bed and the cake layer, which is favorable for the erodibility of the cake formation. The ripples and dunes formations that occurred for the fine sand cake layer induced mass erosion of both the cake layer and the bed due to the wave-induced shear stress (Winterwerp and van Kesteren, 2004). The continuous removal but the high resistance to erosion of the cake layer made of the mixture of fine sediments is explained by the strong interparticle forces among the suspended sediments, avoiding a high resuspension velocity as observed when sediments were tested individually. Our findings indicate an important interaction between the streambed and the suspended sediment size. The smaller the bed particle size, the higher the interaction strength. This behavior is related to the stronger physicochemical forces from small particle sizes acting to preserve the particles joined.

The infiltration velocity never recovered to its initial capacity regardless of the bed shear stress assessed. An overview of cake layer removal and infiltration velocity recovery per sediment type is presented in Table 2. For the homogeneous suspended sediments (clay, silt, fine sand), the infiltration velocity did not show any increase even if the cake layers were partly removed. For the mixed suspended sediments (5% clay, 80% silt, and 15% fine sand), cake layer cracks during the clogging experiments were observed. Therefore, uneven erosion patterns occurred during scouring experiments caused by the presence of the existing cake cracks increasing the longitudinal cracks extent on cake layer formation (Jacobs et al., 2011). Even if a high mobilization of the mixture cake layer during the scouring experiments occurred (Fig. 8), the immediate infiltration velocity recovery is therefore probably associated with preferential flows caused by the ameliorated cake cracking on the surface.

The entrapment of particles in the deeper voids can be considered deep bed clogging and, consequently, there is a reduced chance of natural recovery of infiltration capacity because of the scouring of these particles compared to cake clogging (Goldschneider et al., 2007). In smaller streambed particle sizes, the clogging particles cannot penetrate as deeply, and cake clogging occurs (Brunke, 1999; Veličković, 2005).

It was found that the sediment concentration affected the occurrence of cake and/or deep bed clogging depending on the type of sediment, which in turn influenced the infiltration recovery. Thus, for clay particles the higher concentration favored the cake layer formation limiting the deep bed clogging, while for silt, fine sand and the mixture of sediments the higher sediment concentration, the lower the cake layer formation velocity leading to higher deep bed clogging. The concentration did not show an evident effect on the self-cleansing of the cake layer on sediments other than clay, which suggests that the infiltration recovery was merely a function of deep bed clogging.

5. Conclusions

Based on the presented research it may be concluded that, during (simulated) riverbank filtration, high recovery of the infiltration velocity (84–96%) at low shear stresses was possible for high turbidity water with a mixture of different sediments, as found in natural water bodies. Clay and silt behaved very differently, due to the difference in cohesiveness. Clay was found to produce a persistent sticky cake layer, whereas silt penetrated deeper into the bed, both resulting in an absence of infiltration velocity recovery. The cake layer of fine sand sediments was easiest to remove, resulting in dune formation on the streambed, nevertheless due to deep bed clogging by the sand particles in the coarser streambed the infiltration velocity did not recover. The interaction between the mixed suspended sediments (5% clay, 80% silt, and 15% fine sand), resulted in uneven erosion patterns during scouring of the streambed allowing for the infiltration velocity to recover to 84–96%. Altogether it may be concluded that natural recovery of infiltration capacity during river bank filtration of highly turbid waters is expected to occur, as long as the river carries a mixture of suspended sediments. The fine streambed formation avoids the occurrence of deep bed clogging, which increases the chances of being self-cleaned.

Acknowledgments

The authors would like to acknowledge the support of Colciencias for the scholarship of Juan Pablo Gutiérrez Marín. Special thanks to Eng. Sander de Vree and technicians in the Laboratory for Fluid Mechanics at TU Delft for their assistance during the experimental setup. Recognitions to Jiaxing Fang and Pau Teixidó for their support during the samples collection and analysis. Thanks to the anonymous reviewers for the thorough review, which helped to improve the quality of the article.

Appendix A. Supplementary data

Supplementary data to this article can be found online at https://doi.org/10.1016/j.watres.2018.10.009.

References

Al-Madhhachi, A.T., Hanson, G.J., Fox, G.A., Tyagi, A.K., Bulut, R., 2013. Deriving parameters of a fundamental detachment model for cohesive soils from flume and jet erosion tests. Am. Soc. Agric. Biol. Eng. 56, 489–504. https://doi.org/10.13031/2013.42669.

Baveye, P., Vandevivere, P., Hoyle, B.L., DeLeo, P.C., Sánchez, D. de L., 1998. Environmental impact and mechanisms of the biological clogging of saturated soils and aquifer materials. Crit. Rev. Environ. Sci. Technol. 28, 1–48. https://doi.org/10.1080/10643389891254197.

Blaschke, A.P., Steiner, K.H., Schmalfuss, R., Gutknecht, D., Sengschmitt, D., 2003. Clogging processes in hyporheic interstices of an impounded river, the Danube at Vienna, Austria. Int. Rev. Hydrobiol. 88, 397–413. https://doi.org/10.1002/iroh.200390034.

Bouwer, H., 2002. Artificial recharge of groundwater: hydrogeology and engineering. Hydrogeol. J. 10, 121–142. https://doi.org/10.1007/s10040-001-0182-4.

Brunke, M., 1999. Colmation and depth filtration within streambeds: retention of particles in hypoheic interstices. Int. Rev. Hydrobiol. 84, 99–117. https://doi.org/10.1002/iroh.199900014.

Caldwell, T.G., 2006. Presentation of data for factors significant to yield from several riverbank filtration systems in the U.S. and Europe. In: Hubbs, S.A. (Ed.), Proceedings of the NATO Advanced Research Workshop on Riverbank Filtration Hydrology: Impacts on System Capacity and Water Quality. Bratislava, Slovakia, pp. 299–344. https://doi.org/10.1007/978-1-4020-3938-6_14.

Cunningham, A.B., Anderson, C.J., Bouwer, H., 1987. Effects of sediment-laden flow on channel bed clogging. J. Irrigat. Drain. Eng. 113, 106–118. https://doi.org/10.1061/(ASCE)0733-9437(1987)113:1(106).

CVC, Universidad del Valle, 2004a. Muestreo sedimentológico del material de fondo del río Cauca y principales tributarios. Cali, Colombia.

CVC, Universidad del Valle, 2004b. Caracterización río Cauca. Identificación de parámetros críticos en el río Cauca y sus principales ríos tributarios, tramo Salvajina – La Virginia. Corporación Autónoma Regional del Valle del Cauca, CVC. Proyecto de Modelación del Río Cauca - PMC, Fase II. Volumen IX, Cali, Colombia.

Dawe, M.R., 2006. Assessing Infiltration Velocities during Riverbank Filtration. MScE. Thesis. University of New Brunswick, Fredericton, Canada.

Du, X., Fang, Y., Wang, Z., Hou, J., Ye, X., 2014. The prediction methods for potential suspended solids clogging types during managed aquifer recharge. Water 6, 961–975. https://doi.org/10.3390/w6040961.

Engesgaard, P., Seifert, D., Herrera, P., 2006. Bioclogging in porous media: tracer studies. In: Hubbs, S.A. (Ed.), Proceedings of the NATO Advanced Research Workshop on Riverbank Filtration Hydrology: Impacts on System Capacity and Water Quality. Bratislava, Slovakia, pp. 93–118. https://doi.org/10.1007/978-1-4020-3938-6_5.

Fallah, H., Ahmadi, A., Karaee, M.A., Rabbani, H., 2012. External cake build up at surface of porous medium. Open J. Fluid Dynam. 2, 145–148. https://doi.org/10.4236/ojfd.2012.24015.

Goldberg, S., Forster, H.S., Heick, E.L., 1991. Flocculation of illite/kaolinite and illite/montmorillonite mixtures as affected by sodium adsorption ratio and pH. Clay Clay Miner. 39, 375–380. https://doi.org/10.1346/CCMN.1991.0390406.

Goldschneider, A.A., Haralampides, K.A., MacQuarrie, K.T.B., 2007. River sediment and flow characteristics near a bank filtration water supply: implications for riverbed clogging. J. Hydrol. 344, 55–69. https://doi.org/10.1016/j.jhydrol.2007.06.031.

Grace, M.A., Healy, M.G., Clifford, E., 2016. Performance and surface clogging in intermittently loaded and slow sand filters containing novel media. J. Environ. Manag. 180, 102–110. https://doi.org/10.1016/j.jenvman.2016.05.018.

Gutiérrez, J.P., van Halem, D., Rietveld, L.C., 2016. Particulate matter characterization of Cauca River water in Colombia. In: Hydrology and Earth System Sciences Discussions, pp. 1–20. https://doi.org/10.5194/hess-2016-219.

Huang, J., Hilldale, R.C., Greimann, B.P., 2006. Cohesive sediment transport. In: Yang, C.T. (Ed.), Erosion and Sedimentation Manual. U.S. Department of the Interior, Bureau of Reclamation, Denver, CO, USA, November 2006, pp. 229–282.

Hubbs, S.A., 2006a. Evaluating streambed forces impacting the capacity of riverbed filtration systems. In: Hubbs, S.A. (Ed.), Proceedings of the NATO Advanced Research Workshop on Riverbank Filtration Hydrology: Impacts on System Capacity and Water Quality. Bratislava, Slovakia, pp. 21–42. https://doi.org/10.1007/978-1-4020-3938-6_2.

Hubbs, S.A., 2006b. Changes in riverbed hydraulic conductivity and specific capacity at Louisville. In: Hubbs, S.A. (Ed.), Proceedings of the NATO Advanced Research Workshop on Riverbank Filtration Hydrology: Impacts on System Capacity and Water Quality. Bratislava, Slovakia, pp. 199–220. https://doi.org/10.1007/978-1-4020-3938-6_9.

Jacobs, W., Le Hir, P., Van Kesteren, W.G.M., Cann, P., 2011. Erosion threshold of sand-mud mixtures. Continent. Shelf Res. 31, S14–S25. https://doi.org/10.1016/j.csr.2010.05.012.

Jacobsen, O.H., Moldrup, P., Larsen, C., Konnerup, L., Petersen, L.W., 1997. Particle transport in macropores of undisturbed soil columns. J. Hydrol. 196, 185–203. https://doi.org/10.1016/S0022-1694(96)03291-X.

Julien, P.Y., 1998. Erosion and Sedimentation. Cambridge University Press, Cambridge, UK.

Klassen, I., Hillebrand, G., Olsen, N.R.B., Vollmer, S., Lehmann, B., Nestmann, F., 2013. Flocculation processes and sedimentation of fine sediments in the open annular flume - experiment and numerical modeling. Earth Surf. Dyn. 1, 437–481. https://doi.org/10.5194/esurfd-1-437-2013.

Krishnappan, B.G., 2007. Recent advances in basic and applied research in cohesive sediment transport in aquatic systems. Can. J. Civ. Eng. 34, 731–743. https://doi.org/10.1139/L06-043.

Mahdi, F.M., Holdich, R.G., 2013. Laboratory cake filtration testing using constant rate. Chem. Eng. Res. Des. 91, 1145–1154. https://doi.org/10.1016/j.cherd.2012.11.012.

Manga, M., Beresnev, I., Brodsky, E.E., Elkhoury, J.E., Elsworth, D., Ingebritsen, S.E., Mays, D.C., Wang, C., 2012. Changes in permeability caused by transient stresses: field observations, experiments, and mechanisms. Rev. Geophys. 50 https://doi.org/10.1029/2011RG000382.1.INTRODUCTION.

Martin, R., 2013. Clogging Issues Associated with Managed Aquifer Recharge Methods, IAH Commission on Managing Aquifer Recharge.

Mays, D.C., 2013. Clogging in managed aquifer recharge: flow, geochemistry, and clay colloids. In: Clogging Issues Associated with Managed Aquifer Recharge Methods, pp. 14–24.

Mays, D.C., Hunt, J.R., 2005. Hydrodynamic aspects of particle clogging in porous media. Environ. Sci. Technol. 39, 577–584. https://doi.org/10.1021/es049367k.

Packman, A.I., MacKay, J.S., 2003. Interplay of stream-subsurface exchange, clay particle deposition, and streambed evolution. Water Resour. Res. 39, 1–10. https://doi.org/10.1029/2002WR001432.

Pavelic, P., Dillon, P.J., Mucha, M., Nakai, T., Barry, K.E., Bestland, E., 2011. Laboratory assessment of factors affecting soil clogging of soil aquifer treatment systems. Water Res. 45, 3153–3163. https://doi.org/10.1016/j.watres.2011.03.027.

Pholkern, K., Srisuk, K., Grischek, T., Soares, M., Schäfer, S., Archwichai, L., Saraphirom, P., Pavelic, P., Wirojanagud, W., 2015. Riverbed clogging experiments at potential river bank filtration sites along the Ping River, Chiang Mai, Thailand. Environ. Earth Sci. 73, 7699–7709. https://doi.org/10.1007/s12665-015-4160-x.

Platzer, C., Mauch, K., 1997. Soil clogging in vertical flow reed beds - mechanisms, parameters, consequences and....solutions? Water Sci. Technol. 35, 175–181.

Pugh, C.A., 2008. Sediment transport scaling for physical models. In: García, M.H. (Ed.), Sedimentation Engineering: Processes, Measurements, Modeling, and Practice. American Society of Civil Engineers, pp. 1057–1065.

Reddi, L.N., Xiao, M., Hajra, M.G., Lee, I.M., 2000. Permeability reduction of soil filters due to physical clogging. J. Geotech. Geoenviron. Eng. 126, 236–246. https://doi.org/10.1061/(ASCE)1090-0241(2000)126:3(236).

Ripperger, S., Gösele, W., Alt, C., Loewe, T., 2012. Filtration, 1. Fundamentals. In: Ullmann's Encyclopedia of Industrial Chemistry. John Wiley & Sons, Ltd. https://doi.org/10.1002/14356007.b02, 25.1-2525.40.

Sacramento, R.N., Yang, Y., You, Z., Waldmann, A., Martins, A.L., Vaz, A.S.L., Zitha, P.L.J., Bedrikovetsky, P., 2015. Deep bed and cake filtration of two-size particle suspension in porous media. J. Petrol. Sci. Eng. 126, 201–210. https://doi.org/10.1016/j.petrol.2014.12.001.

Schubert, J., 2003. Water quality improvements with riverbank filtration systems at Düsseldorf waterworks in Germany. In: Ray, C., Melin, G., Linsky, R.B. (Eds.), Riverbank Filtration: Improving Source-water Quality. Kluwer Academic Publishers, New York, Boston, Dordrecht, London, Moscow, pp. 267–277. https://doi.org/10.1007/0-306-48154-5_13.

Schubert, J., 2002. Hydraulic aspects of riverbank filtration—field studies. J. Hydrol. 266, 145–161. https://doi.org/10.1016/S0022-1694(02)00159-2.

Seiler, K.P., Gat, J.R., 2007. Mechanisms and processes of recharge. In: Groundwater Recharge from Run-off, Infiltration and Percolation. Springer, Dordrecht, The Netherlands, pp. 31–67.

Soulsby, R.L., Whitehouse, R.J.S., 1997. Threshold of sediment motion in coastal environments. In: Pacific Coasts and Ports, 1997: Proceedings of the 13th Australasian Coastal and Ocean Engineering Conference and the 6th Australasian Port and Harbour Conference, vol. 1 (Christchurch, New Zeland).

Stuyfzand, P.J., Juhàsz-Holterman, M.H.A., Lange, W.J., 2006. Riverbank filtration in The Netherlands: well fields, clogging and geochemical reactions. In: Hubbs, S.A. (Ed.), Proceedings of the NATO Advanced Research Workshop on Riverbank Filtration Hydrology: Impacts on System Capacity and Water Quality. Bratislava, Slovakia, pp. 119–153. https://doi.org/10.1007/978-1-4020-3938-6_6.

van Rijn, L.C., Walstra, D.-J.R., van Ormondt, M., 2007. Unified view of sediment transport by currents and waves. I: initiation of motion, bed roughness, and bed-load transport. J. Hydraul. Eng. 133, 776–793. https://doi.org/10.1061/(ASCE)0733-9429(2007)133:7(776).

Veličković, B., 2005. Colmation as one of the processes in interaction between the groundwater and surface water. Facta Univ. – Ser. Archit. Civ. Eng. 3, 165–172. https://doi.org/10.2298/FUACE0502165V.

Wang, Z.-Y., 1999. Experimental study on scour rate and river bed inertia. J. Hydraul. Res. 37, 17–37. https://doi.org/10.1080/00221689909498530.

Winterwerp, J.C., van Kesteren, W.G.M., 2004. Introduction to the Physics of Cohesive Sediment in the Marine Environment. Developments in Sedimentology, first ed. ed, vol. 56. Elsevier, Amsterdam, The Netherlands.

Zheng, X.L., Shan, B.B., Chen, L., Sun, Y.W., Zhang, S.H., 2014. Attachment-detachment dynamics of suspended particle in porous media: experiment and modeling. J. Hydrol. 511, 199–204. https://doi.org/10.1016/j.jhydrol.2014.01.039.